Eur J Transl Myol 35 (3) 13952, 2025 doi: 10.4081/ejtm.2025.13952

Shared diagnostic genes and potential mechanisms between asthma and lung cancer revealed by integrated transcriptomic analysis and machine learning

Ling-Jun Zeng, Jun-Cai Tian, Xu Hu, Ting-Ting Zhang, Qing-Qing Dai, Ming-Li Wei

Department of Pulmonary and Critical Care Medicine, West China Hospital of Sichuan University-Ziyang Hospital, Ziyang Central Hospital, Ziyang Sichuan, China.

Abstract

Lung cancer, a severe malignancy with poor prognosis, poses a formidable public health challenge. Beyond conventional risk factors such as smoking, evidence suggests that chronic respiratory diseases also contribute to its development. Among these, asthma, the second most prevalent chronic respiratory condition, is recognized as a risk factor for lung cancer. Nevertheless, the underlying molecular link between these two diseases remains elusive. Our study, leveraging multi-cohort data integration and employing Weighted Gene Co-expression Network Analysis (WGCNA), identified conserved shared genes between lung cancer and asthma. By constructing the functional landscape of these shared genes, we underscored the pivotal roles of pathways related to lung development and cellular metabolic homeostasis in the pathogenesis of both lung cancer and asthma. Utilizing machine learning-based screening, we identified three hub biomarkers: P2RY14, ANXA3, and SLIT2, which could serve as diagnostic tools for these diseases. In summary, our research provides invaluable insights into the shared mechanisms underlying asthma and lung cancer, and potential diagnostic biomarkers.

Key Words: asthma, lung cancer, machine learning.

Eur J Transl Myol 35 (3) 13952, 2025 doi: 10.4081/ejtm.2025.13952

Lung cancer continues to be one of the most significant public health challenges, with a high global incidence and mortality rate. It is the leading cause of cancer-related deaths, accounting for approximately 18% of all cancer fatalities worldwide.[1] Among the various forms of lung cancer, Non-Small-Cell Lung Cancer (NSCLC) stands out as the most common, comprising approximately 85% of all cases. NSCLC encompasses a spectrum of histological subtypes, including adenocarcinoma, squamous cell carcinoma, and large-cell carcinoma, each with distinct pathological and molecular features.[2] Known risk factors for lung cancer include smoking, exposure to environmental pollutants (e.g., asbestos, radon, air pollution), genetic mutations, and various molecular alterations that drive tumorigenesis. However, emerging research has begun to shed light on the potential influence of preexisting respiratory diseases on the development and progression of lung cancer, suggesting a more complex interplay between chronic respiratory conditions and lung cancer risk.[3]

Asthma, the second most prevalent chronic respiratory disease globally, affects over 300 million individuals and presents a growing public health challenge.[4] It is characterized by recurrent episodes of airflow obstruction, bronchial hyper-responsiveness, and inflammation, leading to symptoms such as wheezing, breathlessness, and coughing. These symptoms can worsen during physical exertion, emotional stress, or exposure to allergens. The psychophysiology of asthma is closely linked to chronic airway inflammation, immune dysregulation, and structural changes in the lungs, collectively referred to as airway remodeling.[5,6]

Several epidemiological studies and meta-analyses have established a potential association between asthma and lung cancer, pointing to chronic inflammation as a shared pathological mechanism.[6,7] However, despite this association, the molecular and genetic underpinnings that connect asthma and lung cancer remain poorly understood. The identification of common driver genes, molecular pathways, and biological processes that contribute to both diseases could illuminate the biological relationship between asthma and lung cancer. Furthermore, understanding these shared mechanisms could lead to the development of new diagnostic and therapeutic strategies aimed at mitigating the risk of lung cancer in asthma patients and improving outcomes for both diseases.

In this study, we integrated multiple cohorts of lung cancer and asthma to systematically uncover the shared molecular

mechanisms underlying these diseases. Using weighted gene co-expression network analysis (WGCNA), we identified risk gene modules associated with both conditions. By combining shared Differentially Expressed Genes (DEGs) and common risk module genes, we identified potential driver genes for lung cancer and asthma.

Materials and Methods

Public data sources acquisition and pre-process

The gene expression matrix and corresponding clinical data for lung cancer and asthma were obtained from the Gene Expression Omnibus (GEO, https://www.ncbi.nlm.nih.gov/geo/). Raw data were converted to Transcripts per kilobase Million (TPM) and log2 transformed (TPM+1). Transcriptome microarray data from lung cancer and paired tissues, sourced from GSE116959, GSE43458, and GSE40791, were included in this study. Similarly, transcriptome microarray data for asthma and paired tissues were derived from GSE147878, GSE67472, and GSE41861. Principal Component Analysis (PCA) was conducted to assess batch effects, and the "sva" R package was used to eliminate these effects.

Differential expression genes and Weighted Gene Co-Expression Network Analysis (WGCNA)

To identify Differentially Expressed Genes (DEGs) between the disease group and the control group, we utilized the LIMMA (Linear Models for Microarray Data) package in R. DEGs were defined as genes with an adjusted p-value < 0.05 (using the Benjamini-Hochberg method for multiple testing correction) and a fold change threshold of |log2-FC| >1.[8] Volcano plots were generated to visualize the distribution of DEGs, and heatmaps were produced to highlight expression patterns in both groups. WGCNA (Weighted Gene Co-expression Network Analysis) is a systems biology method that operates without prior knowledge, based on the hypothesis of gene co-expression. It is widely used for identifying new gene modules associated with phenotype. In this study, normalized mRNA expression data was used for WGCNA to identify gene co-expression networks and to correlate gene modules with clinical features (disease vs. control). The analysis for each disease group followed these steps: i) hierarchical clustering was performed using the R package "gplots" to identify outliers in the samples; ii) the "pickSoftThreshold" function was used to select an appropriate soft-thresholding parameter (β) ranging from 1 to 20); iii) the correlation matrix with the optimal β value was transformed into an adjacency matrix, and then into a topological overlap matrix; iv) hierarchical clustering based on average linkage was used to construct a hierarchical clustering tree, followed by the dynamic tree cut algorithm (minModuleSize=30) to identify distinct gene modules. Modules with similar characteristics were merged based on their clustering height; v) gene modules were correlated with clinical phenotype (control, lung cancer, or asthma) using Pearson correlation coefficients. The most phenotype-associated risk modules were then selected.

Pathway enrichment analysis

By combining Differentially Expressed Genes (DEGs) identified through WGCNA with module genes, we were able to identify key genes shared in the pathogenesis of lung cancer and asthma. To explore the biological functions and signaling pathways involved with these genes, we performed Gene Ontology (GO) and Kyoto Encyclopedia of Genes and Genomes (KEGG) pathway enrichment analyses using the "clusterProfiler" R package.[9] The results, with significant enrichment items ($P < 0.05$), are displayed prominently in bar plots.

Identification of hub biomarkers using machine learning

For the identification of disease-specific feature genes using machine learning, we applied SVM modeling through the "MSVM-RFE" package. SVM-RFE (Support Vector Machine-Recursive Feature Elimination) was used to determine the optimal hub genes by sequentially eliminating features in reverse order. In our SVM model, all 39 shared genes were included. The SVM-RFE results were visualized, with red circles representing the points of highest classification accuracy after ten-fold cross-validation. The corresponding gene set reflects the lowest 5×CV error and the highest 5×CV accuracy, representing the most accurate diagnostic markers. Additionally, we employed the "Random Forest" R package to classify important genes through Random Forest (RF). Using the decision tree algorithm, RF analysis identified the most significant variables (genes). By building a random forest model with 500 trees on the discovery cohort and determining the optimal number of trees via cross-validation error, we were able to rank genes by importance. The top 10 most important genes were selected as feature genes for lung cancer or asthma. Finally, we took the intersection of disease-specific feature genes identified by both SVM-RFE and RF for each disease.

Validation of the predictive performance of hub biomarkers in lung cancer and asthma

To evaluate the accuracy of the three hub biomarkers in both the discovery and validation cohorts, the "pROC" package was used to construct ROC curves, and the results were visualized using "ggplot2". The lung cancer discovery cohorts were obtained from GSE116959 and GSE43458, while the validation cohort was sourced from GSE40791. For the asthma group, the discovery cohorts consisted of GSE147878 and GSE67472, and the validation cohort was from GSE41861.

Results

Identification of DEGs in asthma and lung cancer

Given the potential link between asthma and lung cancer, our study initially focused on identifying Differentially Expressed Genes (DEGs) in both conditions. Principal Component Analysis (PCA) of the collected datasets for lung cancer and asthma revealed a significant batch effect across different datasets (Figure 1A-B). To ensure reliable results, we applied the "sva" package to remove these batch effects in both the asthma and lung cancer groups. Subsequent PCA

confirmed that the batch effects had been corrected (Figure 1C-D). We then used the "limma" R package to characterize the DEGs between the two groups. Volcano plots were used to visualize all DEGs in the lung cancer and asthma groups (Figure 1E-F), and the heatmaps illustrated the expression patterns of DEGs within both groups (Figure 1G-H). In brief, the identified DEGs in lung cancer and asthma tissues may contribute to the progression of these diseases, offering insights into their underlying molecular mechanisms.

Screening for key modules by WGCNA

To conduct an unbiased investigation of genes associated with the two diseases mentioned above, in addition to analyzing differentially expressed genes, we also performed Weighted Gene Co-Expression Network Analysis (WGCNA). We constructed gene co-expression networks using the soft-thresholding method. For both disease types, a model fit index greater than 0.85 was considered indicative of a scale-free topology, with the soft-threshold power (β) set to 6. Additionally, a connectivity matrix was generated using the adjacency function (Figure 2A-B). As shown in Figures 2C and 2D, hierarchical clustering was performed using TOM dissimilarity measures. We identified 31 and 44 co-expression modules in lung cancer and asthma samples, respectively. Modules with $p < 0.05$ were considered key modules. As shown in Figure 2E, the MEgreen module, containing 167 genes, exhibited the strongest positive correlation in the lung cancer group. Additionally, the MEdarkred module, which includes 133 genes, showed the strongest positive correlation in the asthma group (Figure 2F). Overall, our analysis identified key gene modules associated with lung cancer and asthma through WGCNA. The genes within these key modules from both groups are likely involved in disease pathogenesis.

Analysis of the shared genes and functional enrichment

To investigate the molecular links between asthma and lung cancer, we focused on identifying core genes that are shared between both conditions. Our approach began by integrating DEGs from asthma and lung cancer datasets, which resulted in the identification of 35 overlapping genes (Figure 3A). Furthermore, to refine our understanding of these shared genes, we employed WGCNA to define risk gene modules for each disease (Figure 3B). By combining these risk gene modules, we identified four additional shared genes, resulting in a total of 39 genes that may play a role in the pathogenesis of both lung cancer and asthma. Next, we sought to investigate the potential biological changes associated with the shared genes between lung cancer and asthma. GO term analysis of the 39 shared genes revealed significant enrichment in lung development-related pathways, such as bronchus development and lung secretory cell differentiation. Additionally, cellular component analysis indicated that the 39 core shared genes are primarily associated with lumen structures (Figure 3C). The results of KEGG pathway enrichment analysis revealed significant enrichment of various metabolic processes, particularly in the context of glutathione metabolism (Figure 3D). These pathways are crucial for the maintenance of normal lung architecture and function, and disruptions in these processes may contribute to both asthma and lung cancer pathogenesis.

Identify potential shared diagnostic genes based on machine learning

For further selection of the most promising candidate diagnostic gene targets with significant potential for classifying the disease and control groups, we applied Support Vector Machine-Recursive Feature Elimination (SVM-RFE) and RF algorithms based on the 39 shared genes. In the lung cancer group, the SVM algorithm identified 21 genes with the lowest 5-fold Cross-Validation (CV) error and the highest 5-fold CV accuracy (Figure 4A-B). Additionally, the 39 shared genes were input into the Random Forest classifier, where the top 10 genes were ranked according to their importance (Figure 4C). By overlapping the results of the SVM-RFE and Random Forest algorithms, we identified 6 shared biomarkers for the lung cancer group (Figure 4D). Similarly, through an integrated machine learning screening process in the asthma group, we identified 8 potential biomarkers (Figure 4E-H).

Diagnostic value and validation of diagnostic hub biomarkers

Based on the machine learning screening of key diagnostic genes for lung cancer and asthma, we further intersected the 6 shared biomarkers identified in lung cancer and the 8 shared biomarkers identified in asthma, yielding 3 hub biomarkers: P2RY14, ANXA3, and SLIT2 (Figure 5A).

First, we analyzed the expression levels of hub biomarkers for lung cancer and asthma in two discovery cohorts. P2RY14 expression was significantly lower in the lung cancer group compared to the control group ($p < 0.0001$), while it was higher in the asthma group ($p < 0.0001$). Similarly, ANXA3 expression was also reduced in the lung cancer group ($p < 0.0001$) and elevated in the asthma group ($p < 0.0001$) Furthermore, SLIT2 showed significantly higher expression in both the lung cancer and asthma groups compared to controls ($p < 0.01$).

The analysis of the validation cohorts further confirmed these findings from the discovery cohorts. We further validated the diagnostic robustness of these hub biomarkers across both training and validation cohorts for lung cancer and asthma. Among these, P2RY14 demonstrated the highest overall diagnostic performance, with ROC values of "0.936", "0.961", "0.763", and "0.744" in the lung cancer training set, lung cancer validation set, asthma training set, and asthma validation set, respectively (Figure 5B). Besides, ANXA3 and SLIT2 also exhibited stable diagnostic performance across four datasets. Among them, ANXA3 demonstrated ROC values of 0.947, 0.951, 0.731, and 0.664 in the lung cancer training set, lung cancer validation set, asthma training set, and asthma validation set, respectively (Figure 5C). Meanwhile, SLIT2 showed ROC values of 0.968, 0.99, 0.728, and 0.695 in the same datasets (Figure 5D). Therefore, the results confirmed their potential as key diagnostic molecules for lung cancer and asthma, respectively.

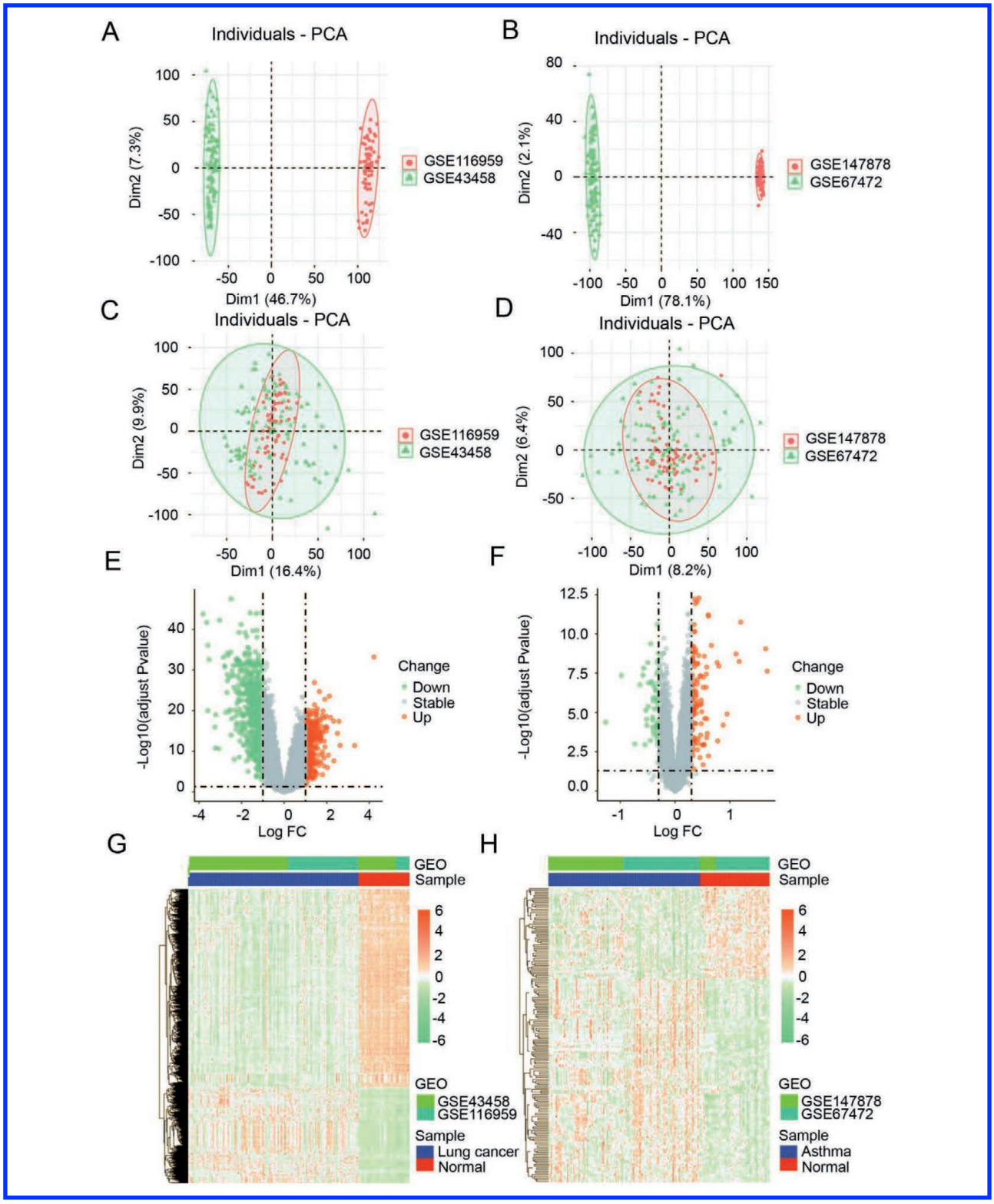

Figure 1. *Identification of DEGs in Asthma and Lung cancer. A, Principle component analysis (PCA) plot of different lung cancer cohorts before Batch Effect Removal; B, PCA plot of different asthma cohorts before Batch Effect Removal; C, PCA plot of different lung cancer cohorts after Batch Effect Removal; D, PCA plot of different asthma cohorts after Batch Effect Removal; E, Volcano plot of Different Expression Genes (DEGs) in lung cancer group compared to control cases; F, Volcano plot of DEGs in asthma group compared to control cases; G, Heatmap of DEGs in the lung cancer group; H, Heatmap of DEGs in the asthma group.*

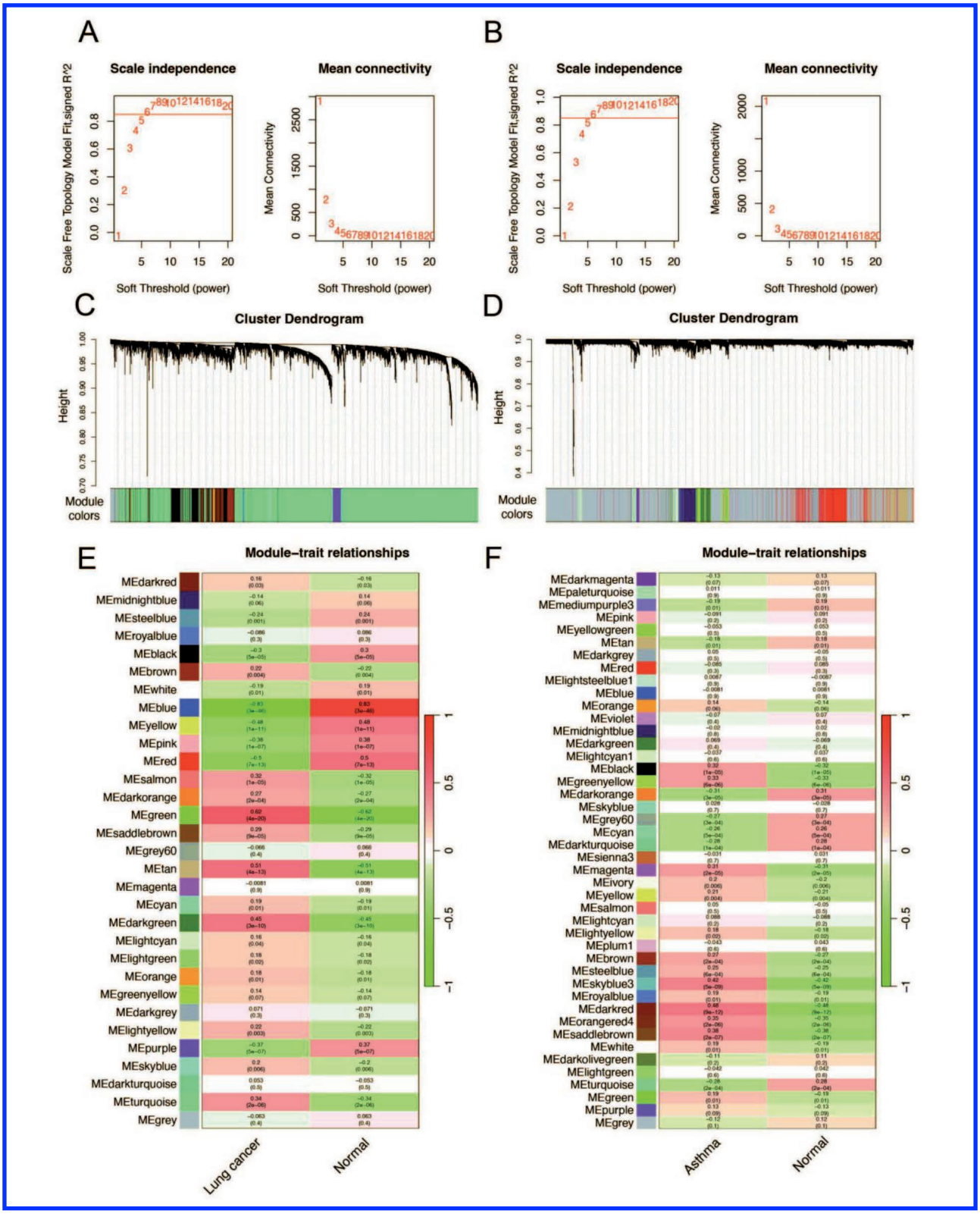

Figure 2. *Screening for key modules by WGCNA. A, Determination of soft-threshold power for lung cancer groups. The left panel illustrates the soft power threshold used to select a scale-free topology model with a fit greater than or equal to 0.85, while the right panel shows the mean connectivity for each soft-threshold value; B, determination of soft-threshold power for asthma groups; C, WGCNA dendrogram plot of 33 modules in lung cancer group; D, WGCNA dendrogram plot of 44 modules in asthma group; E-F, Heatmap of Pearson correlations between different modules and phenotype.*

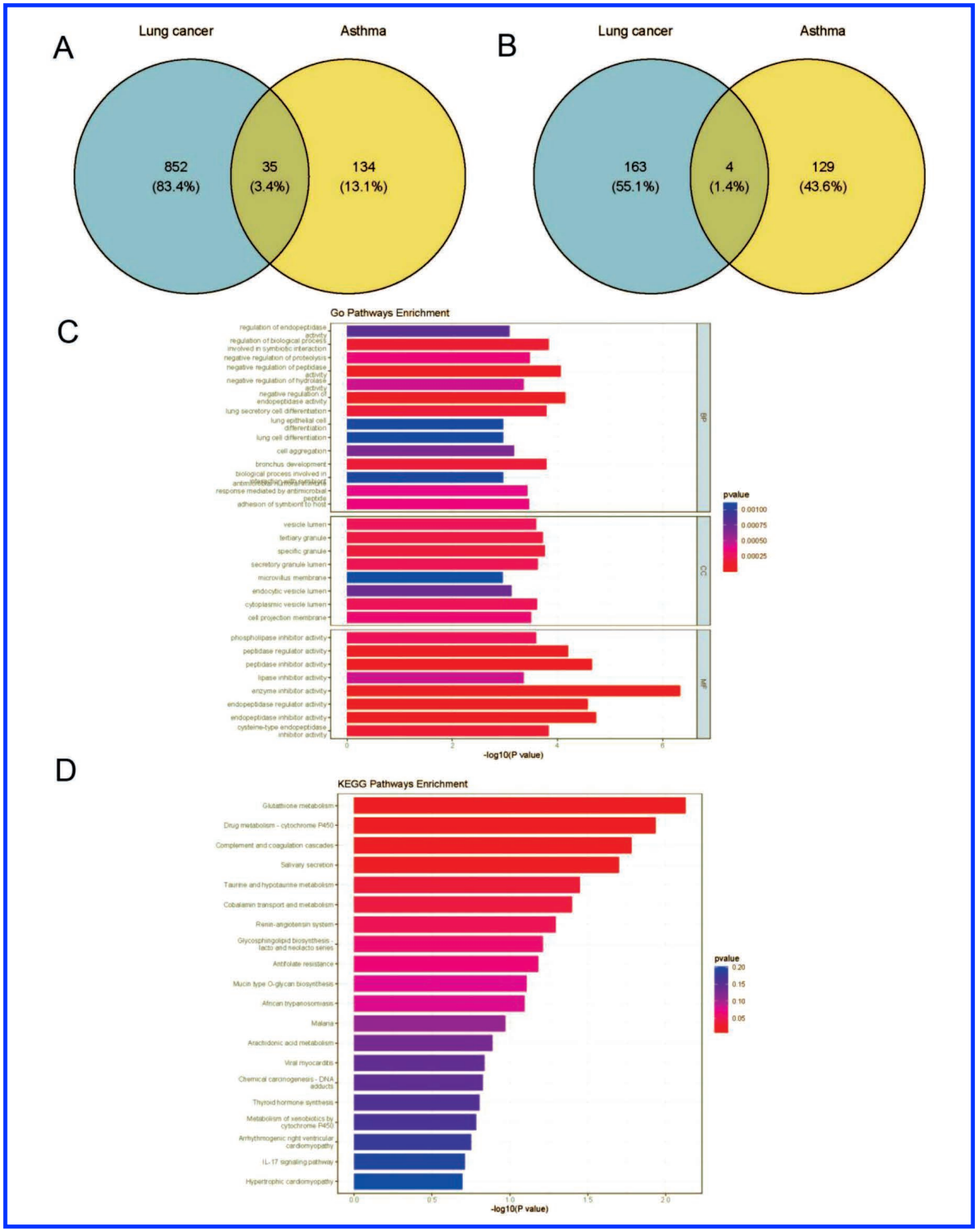

Figure 3. *Analysis of the shared genes and functional enrichment. A, The Venn diagram shows the overlap of DEGs between lung cancer and asthma groups; B, the Venn plot illiterates the overlap of module genes between lung cancer and asthma groups.; C, Gene Ontology (GO) analysis of the 39 shared genes of lung cancer and asthma; D, KEGG pathways enrichment analysis of the 39 shared genes.*

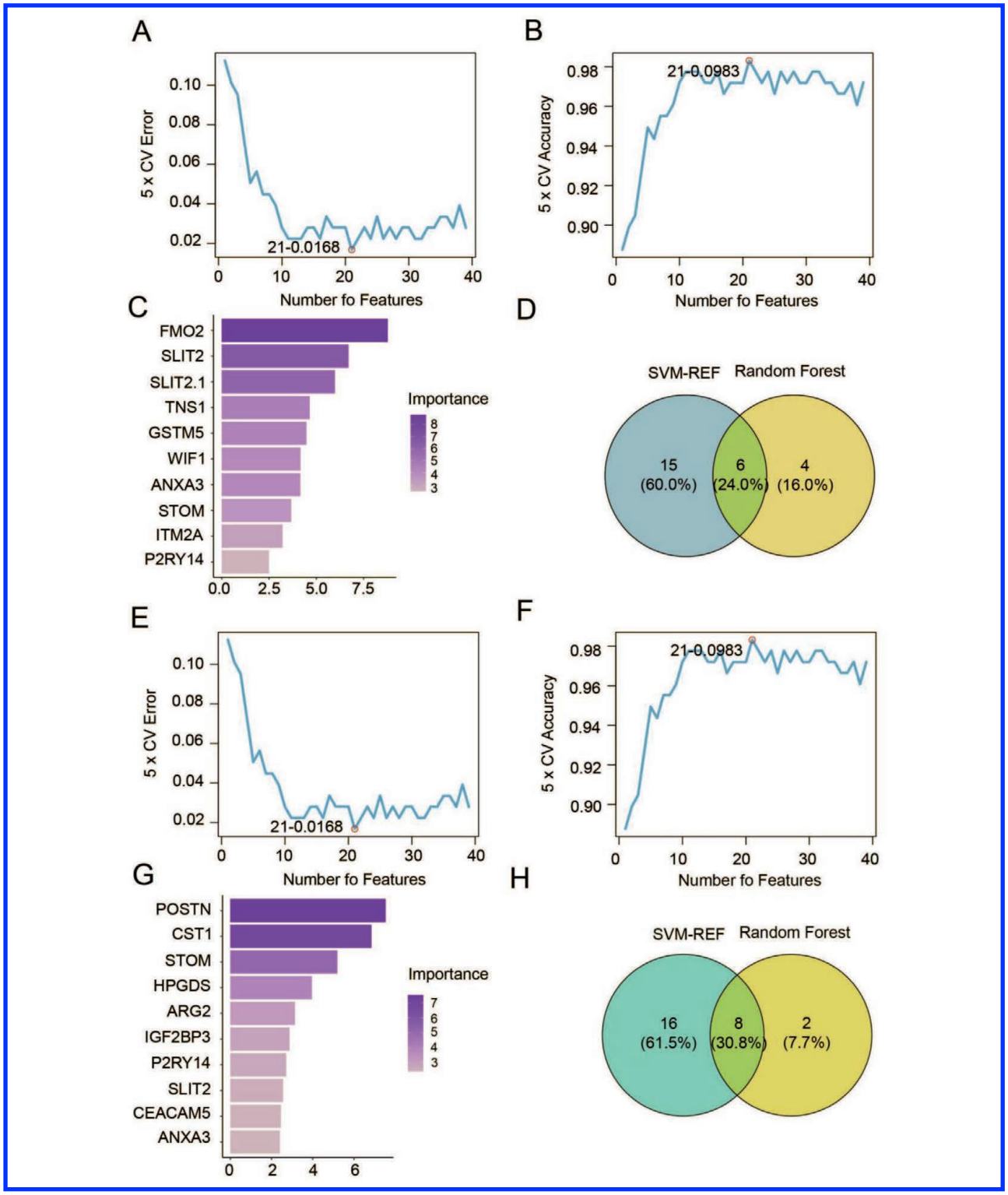

Figure 4. *Identify potential shared diagnostic genes based on machine learning. A, SVM-RFE error plot of lung cancer group. This line plot shows the 5-fold cross-validation (CV) error decreasing as the number of features increases. The best performance (minimum error of 0.0168) occurs when 21 features are used; B, accuracy Plot for SVM-RFE in lung cancer group. The highest accuracy (0.983) is achieved at 21 features; C, barplot of top 10 genes ranked by importance in lung cancer group; D, overlap of shared biomarkers identified by SVM-RFE and RF; E, the 5-fold CV error curve for RF in the asthma group; F, the 5-fold CV accuracy curve for RF in the asthma group; G, Venn diagram displaying the overlap of genes identified by SVM-RFE and Random Forest in the asthma group.*

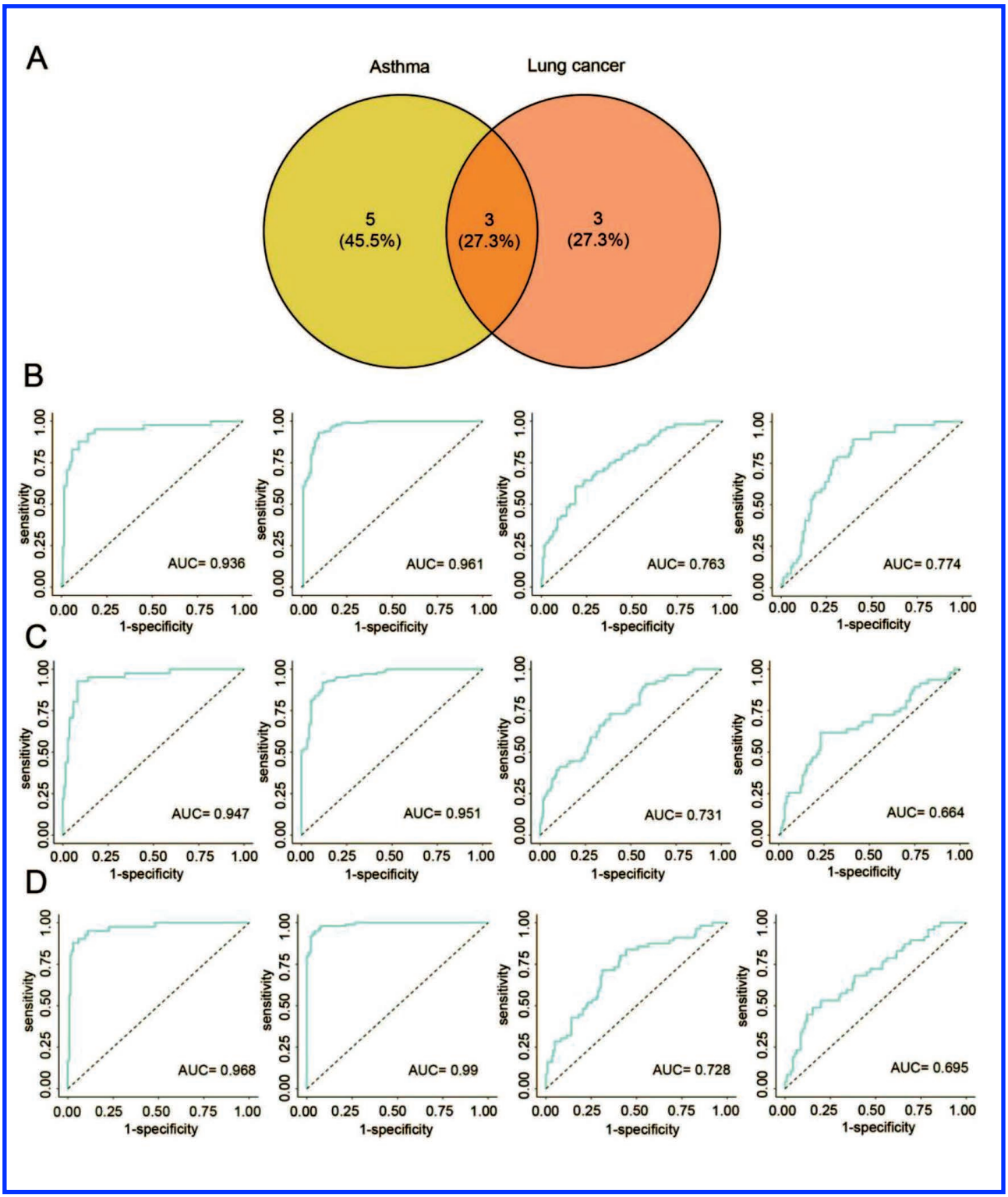

Figure 5. *Diagnostic value and validation of diagnostic hub biomarkers. A, The Venn diagram of the intersection of hub biomarkers across the two diseases; B, AUC plot for Diagnostic Performance of P2RY14 (From left to right are the lung cancer training set, lung cancer validation set, asthma training set, and asthma validation set, respectively); C, the AUC plot illustrates the diagnostic performance of the ANXA3 in lung cancer and asthma. (From left to right are the lung cancer training set, lung cancer validation set, asthma training set, and asthma validation set, respectively), D, the AUC plot for SLIT2 displays its diagnostic performance. From left to right, the plot represents the lung cancer training set, lung cancer validation set, asthma training set, and asthma validation set.*

Discussion

Lung cancer and asthma are both respiratory diseases that pose significant challenges to public health. Given the carcinogenic role of chronic respiratory diseases in lung cancer, investigating the shared mechanisms and disease markers between asthma and lung cancer can enhance our understanding of the crosstalk between these conditions. Asthma is a common chronic respiratory disease that typically leads to airflow limitation during its active phase.[10] A Mendelian randomization study by Zhang *et al.* suggested that airflow restriction could be an independent predictor of Lung Squamous Cell Carcinoma (LUSC).[11] Moreover, a recent meta-analysis, reviewing 24 population-based cohort studies involving 1,072,502 patients, confirmed a significant association between asthma and an increased risk of lung cancer across all individuals (OR=1.29, 95% CI 1.19-1.38). Further Mendelian randomization analysis also supported a causal relationship between asthma and lung cancer (OR=1.11, 95% CI 1.04-1.17, P=.0008).[6] Despite the clear clinical association between lung cancer and asthma, the molecular crosstalk between the two diseases remains elusive.

Here, by integrating multiple lung cancer and asthma cohorts, we identified shared molecular factors between the two diseases using high-throughput sequencing data. Our analysis combined differential gene expression analysis and an unbiased systematic screening through WGCNA. Ultimately, we identified 39 shared genes.

Pathway enrichment analysis was further conducted based on the 39 shared genes. The results of the GO pathway enrichment analysis revealed significant enrichment in lung-related developmental processes, including lung cell differentiation, lung epithelial cell differentiation, and bronchus development. Additionally, molecular function analysis of the 39 shared genes indicated significant activation of various enzyme inhibitor activities, including those related to lipase and enzyme inhibition. These findings suggest that dysfunction in respiratory cell functions is a common feature of both diseases.

Chronic airway inflammation can lead to alterations in the bronchial epithelium and lung microenvironment, disrupting respiratory homeostasis and creating conditions that promote a carcinogenic environment in the lungs.[12,13] For example, inflammation can induce the up-regulation of cyclooxygenase-2 (COX-2) in Non-Small-Cell Lung Cancer (NSCLC), where it plays a critical role in promoting Epithelial-Mesenchymal Transition (EMT).[14] Additionally, various metabolic processes have been shown to play critical roles in both asthma and lung cancer. For example, cysteine levels and glutathione biosynthesis are significantly increased in KRAS Mutant Lung Adenocarcinoma (LUAD). This type of metabolic reprogramming is believed to contribute to the tumor progression of LUAD.[15] Additionally, cytochrome P450-related metabolism is also thought to be associated with lung cancer development. CYP1 enzymes, as key intermediates in the metabolism of various carcinogens, regulate the production of reactive metabolites that form DNA adducts, leading to genomic mutations.[16] Similarly, elevated total GSH levels in blood samples from asthma patients reflect the systemic inflammatory component of the disease. Additionally, several antioxidant enzymes involved in maintaining the GSH/GSSG ratio, as well as enzymes that utilize GSH, have been found to undergo significant changes in the lungs and blood of asthma patients.[17] These evidences indicate that metabolic homeostasis could play a pivotal role in the molecular interplay between lung cancer and asthma. Our KEGG pathway enrichment analysis of the 39 shared genes in both diseases further highlights the significance of metabolic homeostasis, particularly glutathione metabolism. These findings suggest that glutathione metabolism serves as a critical link between asthma and lung cancer.

To further narrow down the hub biomarkers, we applied machine learning screening to the 39 shared genes. Our screening strategy combined SVM-RFE and RF algorithms. By intersecting the results, we ultimately identified three hub biomarkers as diagnostic markers for both asthma and lung cancer: P2RY14, ANXA3, and SLIT2. Their diagnostic performance was validated across multiple cohorts, confirming their robustness. Our expression analysis of the aforementioned genes revealed that SLIT2 is significantly downregulated in both lung cancer and asthma, while P2RY14 and ANXA3 are downregulated in lung cancer but upregulated in asthma. This highlights the conserved functional role of SLIT2 in both lung cancer and asthma.

Slit Guidance Ligand 2 (SLIT2) is an evolutionarily conserved secreted glycoprotein that regulates the directed migration (chemotaxis) of various cell types, from leukocytes to cancer cells.[18] Limited evidence suggests that SLIT2 acts as a tumor suppressor in lung cancer, inhibiting disease progression, which aligns with our analysis.[19] Although SLIT2 has not been studied extensively in asthma, research has shown that fibroblast-secreted SLIT2 can suppress lung fibrosis.[20] Since asthma can lead to fibrosis during its progression, the potential role of SLIT2 in asthma-related fibrosis warrants further investigation.

Conclusions

In summary, our study integrated multiple lung cancer and asthma cohorts and employed a range of bioinformatics approaches to identify shared genes between these two diseases. The shared pathway analysis highlighted the critical role of cellular and metabolic homeostasis, particularly glutathione metabolism, in the coordinated progression of both lung cancer and asthma. Finally, through machine learning, we identified three hub biomarkers for the diagnosis of lung cancer and asthma. Our research offers unique molecular insights into the pathogenesis of these diseases and supports the development of precision diagnostics and treatments for lung cancer and asthma.

Funding

This work was supported by Special Scientific Research Project on Wounds/Chronic Diseases (Tigecycline) of Sichuan Medical Association (No. 2024TG53), Science and Technology Plan Project of Ziyang (No. zykjjsc20-yyjc-2023-09)

Conflict of interest

The authors declare that the research was conducted in the absence of any commercial or financial relationships that could be construed as a potential conflict of interest.

Ethics approval

As this research is an integrated transcriptomic analysis and machine learning manuscript, so no need for confirmation by the Ethics Committee of the university.

Informed consent

All patients participating in this study signed a written informed consent form for participating in this study.

Patient consent for publication

Written informed consent was obtained from a legally authorized representative(s) for anonymized patient information to be published in this article.

Availability of data and materials

All data generated or analyzed during this study are included in this published article.

Corresponding author

Ming-Li Wei, Department of Pulmonary and Critical Care Medicine, West China Hospital of Sichuan University-Ziyang Hospital, Ziyang Central Hospital, Ziyang Sichuan, 641300, China.
ORCID ID: 0000-0003-1441-9489
E-mail: 316987601@qq.com

Co-authors

Ling-Jun Zeng
ORCID ID: 0009-0004-8531-7580
E-mail: zenglj2019@163.com

Jun-Cai Tian
ORCID ID: 0009-0002-7077-5023
E-mail: 364775747@qq.com

Xu Hu
ORCID ID: 0009-0003-4291-998X
E-mail: 928664145@qq.com

Ting-Ting Zhang
ORCID ID: 0009-0003-5977-0317
E-mail: 244221002@qq.com
Qing-Qing Dai
ORCID ID: 0009-0004-5373-585X
E-mail: 1901541349@qq.com

References

1. Sung H, Ferlay J, Siegel RL, et al. Global Cancer Statistics 2020: GLOBOCAN Estimates of Incidence and Mortality Worldwide for 36 Cancers in 185 Countries. CA Cancer J Clin 2021;71:209-49.
2. Herbst RS, Morgensztern D, Boshoff C. The biology and management of non-small cell lung cancer. Nature 2018;553:446-54.
3. Bade BC, Dela Cruz CS. Lung Cancer 2020: Epidemiology, etiology, and prevention. Clin Chest Med 2020; 41:1-24.
4. GBD Chronic Respiratory Disease Collaborators. Prevalence and attributable health burden of chronic respiratory diseases, 1990-2017: a systematic analysis for the Global Burden of Disease Study 2017. Lancet Respir Med 2020;8:585-96.
5. Huang JY, Jian ZH, Nfor ON, et al. The effects of pulmonary diseases on histologic types of lung cancer in both sexes: a population-based study in Taiwan. BMC Cancer 2015;15:834.
6. Huang Q, Huang Y, Xu S, et al. Association of asthma and lung cancer risk: A pool of cohort studies and Mendelian randomization analysis. Medicine (Baltimore) 2024;103:e35060.
7. Dadgar-Zankbar L, Mokhtaryan M, Bafandeh E, et al. Microbiome and bladder cancer: the role of probiotics in treatment. Future Microbiol 2025;20:73-90.
8. Ritchie ME, Phipson B, Wu D, et al. limma powers differential expression analyses for RNA-sequencing and microarray studies. Nucleic Acids Res 2015; 43:e47.
9. Wu T, Hu E, Xu S, et al. clusterProfiler 4.0: A universal enrichment tool for interpreting omics data. Innovation (Camb) 2021;2:100141.
10. Papi A, Brightling C, Pedersen SE, et al. Asthma. Lancet 2018;391:783-800.
11. Zhang Q, Cai G, Cui F, et al. The relationship of airflow limitation with lung squamous cell carcinoma: evidence from mendelian randomization analysis. J Cancer Res Clin Oncol 2023;149:6999-7006.
12. Engels EA. Inflammation in the development of lung cancer: epidemiological evidence. Expert Rev Anticancer Ther 2008;8:605-15.
13. Lee G, Walser TC, Dubinett SM. Chronic inflammation, chronic obstructive pulmonary disease, and lung cancer. Curr Opin Pulm Med 2009;15:303-7.
14. Khuri FR, Wu H, Lee JJ, et al. Cyclooxygenase-2 overexpression is a marker of poor prognosis in stage I non-small cell lung cancer. Clin Cancer Res 2001;7:861-7.
15. Hu K, Li K, Lv J, et al. Suppression of the SLC7A11/glutathione axis causes synthetic lethality in KRAS-mutant lung adenocarcinoma. J Clin Invest 2020;130: 1752-66.
16. Stading R, Gastelum G, Chu C, et al. Molecular mechanisms of pulmonary carcinogenesis by Polycyclic Aromatic Hydrocarbons (PAHs): Implications for human lung cancer. Semin Cancer Biol 2021;76:3-16.
17. Reynaert NL. Glutathione biochemistry in asthma. Biochim Biophys Acta 2011;1810:1045-51.
18. Bhosle VK, Tan JM, Li T, et al. SLIT2/ROBO1 signal-

ing suppresses mTORC1 for organelle control and bacterial killing. Life Sci Alliance 2023;6:e202301964.
19. Wang J, Ye J, Dang Y, et al. LncRNA PGM5-AS1 inhibits non-small cell lung cancer progression by targeting miRNA-423-5p/SLIT2 axis. Cancer Cell Int 2024; 24:216.
20. Pilling D, Zheng Z, Vakil V, et al. Fibroblasts secrete Slit2 to inhibit fibrocyte differentiation and fibrosis. Proc Natl Acad Sci U S A 2014;111:18291-6.

Disclaimer

Submitted: 5 May 2025.
Accepted: 26 May 2025.
Early access: 27 August 2025.